

# A millisecond pulsar in a stellar triple system

S. M. Ransom<sup>1</sup>, I. H. Stairs<sup>2</sup>, A. M. Archibald<sup>3,4</sup>, J. W. T. Hessels<sup>3,5</sup>, D. L. Kaplan<sup>6,7</sup>, M. H. van Kerkwijk<sup>8</sup>, J. Boyles<sup>9,10</sup>, A. T. Deller<sup>3</sup>, S. Chatterjee<sup>11</sup>, A. Schechtman-Rook<sup>7</sup>, A. Berndsen<sup>2</sup>, R. S. Lynch<sup>4</sup>, D. R. Lorimer<sup>9</sup>, C. Karako-Argaman<sup>4</sup>, V. M. Kaspi<sup>4</sup>, V. I. Kondratiev<sup>3,12</sup>, M. A. McLaughlin<sup>9</sup>, J. van Leeuwen<sup>3,5</sup>, R. Rosen<sup>1,9</sup>, M. S. E. Roberts<sup>13,14</sup>, K. Stovall<sup>15,16</sup>

Published online by *Nature* on 2014 January 5. DOI: 10.1038/nature12917

<sup>1</sup>National Radio Astronomy Observatory, Charlottesville, VA, USA

<sup>2</sup>Dept. of Physics and Astronomy, University of British Columbia, Vancouver, BC, Canada

<sup>3</sup>Netherlands Institute for Radio Astronomy (ASTRON), Dwingeloo, The Netherlands

<sup>4</sup>Dept. of Physics, McGill University, Montreal, QC, Canada

<sup>5</sup>Astronomical Institute “Anton Pannekoek,” Univ. of Amsterdam, Amsterdam, The Netherlands

<sup>6</sup>Physics Dept., University of Wisconsin-Milwaukee, Milwaukee, WI, USA

<sup>7</sup>Dept. of Astronomy, University of Wisconsin-Madison, Madison, WI, USA

<sup>8</sup>Dept. of Astronomy and Astrophysics, University of Toronto, Toronto, ON, Canada

<sup>9</sup>Dept. of Physics and Astronomy, West Virginia University, Morgantown, WV, USA

<sup>10</sup>Physics and Astronomy Dept., Western Kentucky University, Bowling Green, KY, USA

<sup>11</sup>Center for Radiophysics and Space Research, Cornell University, Ithaca, NY, USA

<sup>12</sup>Astro Space Center of the Lebedev Physical Institute, Moscow, Russia

<sup>13</sup>Eureka Scientific Inc., Oakland, CA, USA

<sup>14</sup>Physics Dept., New York University at Abu Dhabi, Abu Dhabi, UAE

<sup>15</sup>Physics Dept., University of Texas at Brownsville, Brownsville, TX, USA

<sup>16</sup>Physics and Astronomy Dept., University of New Mexico, Albuquerque, NM, USA

**Gravitationally bound three-body systems have been studied for hundreds of years<sup>1,2</sup> and are common in our Galaxy<sup>3,4</sup>. They show complex orbital interactions, which can constrain the compositions, masses, and interior structures of the bodies<sup>5</sup> and test theories of gravity<sup>6</sup>, if sufficiently precise measurements are available. A triple system containing a radio pulsar could provide such measurements, but the only previously known such system, B1620–26<sup>7,8</sup> (with a millisecond pulsar, a white dwarf, and a planetary-mass object in an orbit of several decades), shows only weak interactions. Here we report precision timing and multi-wavelength observations of PSR J0337+1715, a millisecond pulsar in a hierarchical triple system with two other stars. Strong gravitational interactions are apparent and provide the masses of the pulsar ( $1.4378(13) M_{\odot}$ , where  $M_{\odot}$  is the solar mass and the parentheses contain the uncertainty in the final decimal places) and the two white dwarf companions ( $0.19751(15) M_{\odot}$  and  $0.4101(3) M_{\odot}$ ), as well as the inclinations of the orbits (both  $\sim 39.2^{\circ}$ ). The unexpectedly coplanar and nearly circular orbits indicate a complex and exotic evolutionary past that differs from those of known stellar systems. The gravitational field of the outer white dwarf strongly accelerates the inner binary containing the neutron star, and the system will thus provide an ideal laboratory in which to test the strong equivalence principle of general relativity.**

Millisecond pulsars (MSPs) are neutron stars that rotate hundreds of times per second and emit radio waves in a lighthouse-like fashion. They are thought to form in binary systems<sup>9</sup> and their rotation rates and orbital properties can be measured with exquisite precision via the unambiguous pulse-counting methodology known as pulsar timing. As part of a large-scale pulsar survey<sup>10,11</sup> with the Green Bank Telescope (GBT), we have discovered the only known MSP in a stellar triple system. The pulsar has a spin period of 2.73 ms, is relatively bright ( $\sim 2$  mJy at 1.4 GHz), and has a complex radio pulse profile with multiple narrow components.

Though initial timing observations showed a seemingly typical binary MSP system with a 1.6-day circular orbit and a  $0.1\text{--}0.2 M_{\odot}$  white dwarf (WD) companion, large timing systematics quickly appeared, strongly suggesting the presence of a third body. There are two other MSPs known to have multiple companions: the famous pulsar B1257+12 which hosts at least 3 low-mass planets<sup>12,13</sup>, and the MSP triple system B1620–26 in globular cluster M4 with a WD inner companion and a roughly Jupiter-mass outer companion<sup>7,8</sup>. The timing perturbations from J0337+1715 were much too large to be caused by a planetary mass companion.

We began an intensive multi-frequency radio timing campaign (Methods) using the GBT, the Arecibo telescope, and the Westerbork Synthesis Radio Telescope (WSRT) to constrain the system’s position, orbital parameters, and the nature of the third body. At Arecibo, we achieve median arrival time uncertainties of  $0.8 \mu\text{s}$  in 10 seconds, implying that half-hour integrations provide  $\sim 100$  ns precision, making J0337+1715 one of the highest-timing-precision MSPs known.

To fold the pulsar signal we approximate the motion of J0337+1715 using a pair of Keplerian orbits, with the centre of mass of the inner orbit moving around in the outer orbit. We determine pulse times of arrival (TOAs) from the folded radio data using standard techniques (Methods) and then correct them to the Solar System barycentre at infinite frequency using a precise radio position obtained with the Very Long Baseline Array (VLBA; Methods). These TOAs vary significantly compared to a simple pulsar spin-down model by the Rømer and Einstein delays<sup>14</sup>. The Rømer delay is a simple geometric effect due to the finite speed of light and therefore measures the pulsar’s orbital motion. Its amplitude is  $a_I \sin i/c \sim 1.2$  sec for the inner orbit and  $\sim 74.6$  sec for the outer orbit (see Figures 1 and 2).

The Einstein delay is the cumulative effect of time dilation, both special-relativistic due to the transverse Doppler effect, and general-relativistic via gravitational redshift due to the pulsar’s position in the total gravitational potential of the system. For J0337+1715, the gravitational redshift portion is covariant with fitting the projected semimajor axis of the orbit just as the full Einstein delay is for other pulsars with circular orbits. The transverse Doppler effect is easily measurable, though, since it is proportional to  $v^2/c^2 = |\mathbf{v}_I + \mathbf{v}_O|^2/c^2 = (v_I^2 + v_O^2 + 2\mathbf{v}_I \cdot \mathbf{v}_O)/c^2$ , where  $\mathbf{v}_I$  and  $\mathbf{v}_O$  are the 3-dimensional velocities in the inner and outer orbit, respectively, and  $v_I$  and  $v_O$  the corresponding speeds. The  $v^2$  terms are covariant with orbital fitting as in the binary case, but the cross term  $\mathbf{v}_I \cdot \mathbf{v}_O/c^2$  contributes delays of tens of  $\mu\text{s}$  on the timescale of the inner orbit.

The two-Keplerian-orbit approximation results in systematic errors of up to several hundred  $\mu\text{s}$  over multiple timescales due to unmodeled three-body interactions (see Figure 1), but those sys-

tematics carry a great deal of information about the system masses and geometry. The planet pulsar B1257+12 showed similar systematics<sup>12</sup> and direct numerical integrations confirmed their planetary nature and provided the masses and orbits of the planets<sup>13,15</sup>. The interactions in J0337+1715 are many orders of magnitude stronger, but they, along with the Rømer and Einstein delays, can be similarly modeled by direct integration.

We use Monte Carlo techniques (Methods) to find sets of parameter values that minimize the difference between measured TOAs and predicted TOAs from three-body integrations, and we determine their expected values and error estimates directly from the parameter posterior distributions. We plot the results in Figure 1 and list best-fit parameters and several derived quantities in Table 1. Component masses and relative inclinations are determined at the 0.1–0.01% level, one to two orders of magnitude more precisely than from other MSP timing experiments, in what is effectively a gravitational-theory-independent way. A detailed description of the three-body model and fitting procedure is under way (A.M.A. *et al.*, manuscript in preparation).

Based on an early radio position, we identified an object with unusually blue colours in the Sloan Digital Sky Survey (SDSS; Figure 3)<sup>16</sup>. The optical plus archival ultraviolet photometry, combined with new near- and mid-infrared photometry, are consistent (Methods) with a single  $\sim 15,000$  K WD, which optical spectroscopy confirmed is the inner WD in the system (D.L.K. *et al.*, manuscript in preparation). When combined with the known WD mass from timing, WD models provide a radius allowing us to infer a photometric distance to the system of  $1,300 \pm 80$  pc. The photometry and timing masses also exclude the possibility that the outer companion is a main sequence star.

The pulsar in this system appears to be a typical radio MSP, but it is unique in having two WD companions in hierarchical orbits. While more than 300 MSPs are known in the Galaxy and in globular clusters, J0337+1715 is the first MSP stellar triple system found. As there are no significant observational selection effects discriminating against the discovery of pulsar triple (as opposed to binary) systems, this implies that  $\lesssim 1\%$  of the MSP population resides in stellar triples and that  $\lesssim 100$  such systems exist in the Galaxy.

Predictions for the population of MSP stellar triples have suggested most would have highly eccentric outer orbits due to dynamical interactions between the stars during stellar evolution<sup>17</sup>. Such models can also produce eccentric binaries like MSP J1903+0327<sup>18</sup>, if the inner WD, which had previously recycled the pulsar, was destroyed or ejected from the system dynamically<sup>19</sup>. In these situations, however, the co-planarity and circularity of the orbits of J0337+1715 would be very surprising. Those orbital characteristics, and their highly hierarchical nature ( $P_{b,O}/P_{b,I} \sim 200$ ), imply that the current configuration is stable on long timescales<sup>20</sup>, greatly increasing the odds of observing a triple system like J0337+1715. Secular changes to the various orbital parameters will occur in the long term<sup>21</sup>, however, and the three-body integrations and timing observations will predict and measure them.

The basic evolution of the system, which was almost certainly complex and exotic, may have progressed as follows. The most massive of the progenitor stars evolved off the main-sequence and

exploded in a supernova, creating the neutron star. At least two of the companions to the original primary survived the explosion, probably in eccentric orbits. After of-order  $10^9$  years, the outermost star, the next most massive, evolved and transferred mass onto the inner binary, comprising the neutron star and a lower mass main sequence star, perhaps within a common envelope. During this phase, the angular momentum vectors of the inner and outer orbits were torqued into near alignment<sup>22</sup>. After the outer star ejected its envelope to become a WD and another of-order  $10^9$  years passed, the remaining main-sequence star evolved and recycled the neutron star via the standard scenario<sup>23</sup>. During this phase, the inner orbit became highly circular but only a small amount of mass ( $<0.2 M_{\odot}$ , in total) was transferred to the neutron star: enough to drastically increase its rotation rate, but not enough to make it particularly massive<sup>24,25</sup>. Since then, secular effects due to three-body interactions have aligned the apsides of the two orbits<sup>5</sup>, although our three-body integrations display librations around apsidal alignment on both outer-orbital and secular timescales. This scenario nicely explains the co-planarity and circularity of the orbits as well as the fact that both WD companions fall on the predicted He-WD-mass vs. orbital period relation<sup>23</sup>.

Perhaps the most interesting aspect of J0337+1715 is its potential to provide extremely sensitive tests of the strong equivalence principle (SEP)<sup>26,27</sup>, a key implication of which is that the orbital motions of bodies with strong self-gravity are the same as those with weak self-gravity. In the case of J0337+1715, a neutron star with a gravitational binding energy  $3GM/5Rc^2 \sim 0.1$  and a low-mass WD with much smaller gravitational binding energy ( $\sim 3 \times 10^{-6}$ ) are both falling in the relatively strong gravitational potential of the outer WD. The five orders of magnitude difference in the gravitational binding energies of the pulsar and WD, as well as the large absolute value for the pulsar, provide a much larger “lever arm” for testing the SEP than Solar System tests, where the planets and moons have gravitational binding energies between  $10^{-11}$  and  $10^{-9}$ . Previous strong-field SEP tests used MSP–WD systems and the Galactic field as the external perturbing field<sup>28,29</sup>. In the case of J0337+1715, the perturbing field (that of the outer WD) is 6–7 orders of magnitude larger, greatly magnifying any possible SEP violation effects<sup>26,27</sup>. Since most metric theories of gravity besides general relativity predict violations of the SEP at some level, high-precision timing of J0337+1715 should soon produce unique and extremely interesting new tests of gravity<sup>26</sup>.

## METHODS SUMMARY

We have taken many hundreds of hours of radio timing observations with the GBT, Arecibo, and WSRT over the last two years, with the best observations having time-of-arrival uncertainties of  $0.8 \mu\text{s}$  in 10 s of data. These TOAs are fit using a high-precision numerical integrator, including Newtonian gravitational effects from the three-body interactions as well as special-relativistic transverse Doppler corrections and general-relativistic Einstein and Shapiro delays (the last two are not yet important for the fitting). Uncertainties on the fitted parameters are derived using Markov chain Monte Carlo (MCMC) techniques.

The optical/ultraviolet/infrared photometry of the inner object were fit using an absorbed WD atmosphere, finding results very close to the spectroscopic values. Based on the spectroscopic gravity, the photometric radius of the inner WD is  $0.091 \pm 0.005 R_{\odot}$  which leads to a photometric

distance to the system. We see no emission from the outer object, and can reject all single or binary main-sequence stars as being the outer companion. The data are consistent with a  $0.4 M_{\odot}$  WD.

The radio timing fits benefitted from a radio interferometric position of J0337+1715 determined from a 3-hour observation with the VLBA. The absolute positional accuracy is estimated to be 1–2 milli-arcsec. A series of observations which has already begun will determine the parallax distance to 1–2% precision as well as the  $237/D_{\text{kpc}}$   $\mu$ -arcsec reflex motion on the sky caused by the outer orbit, where  $D_{\text{kpc}}$  is the distance to the system in kpc.

1. Newton, I. *Philosophiae naturalis principia mathematica* (J. Societatis Regiae ac Typis J. Streater, 1687).
2. Gutzwiller, M. C. Moon-Earth-Sun: The oldest three-body problem. *Reviews of Modern Physics* **70**, 589–639 (1998).
3. Tokovinin, A., Thomas, S., Sterzik, M. & Udry, S. Tertiary companions to close spectroscopic binaries. *A&A* **450**, 681–693 (2006). [arXiv:astro-ph/0601518](https://arxiv.org/abs/astro-ph/0601518).
4. Rappaport, S. *et al.* Triple-star Candidates among the Kepler Binaries. *ApJ* **768**, 33 (2013). [1302.0563](https://arxiv.org/abs/1302.0563).
5. Fabrycky, D. C. Non-Keplerian Dynamics of Exoplanets. In Seager, S. (ed.) *Exoplanets*, 217–238 (University of Arizona Press, Tuscon, AZ, 2011).
6. Kopeikin, S. & Vlasov, I. Parametrized post-Newtonian theory of reference frames, multipolar expansions and equations of motion in the N-body problem. *Phys. Rep.* **400**, 209–318 (2004). [arXiv:gr-qc/0403068](https://arxiv.org/abs/gr-qc/0403068).
7. Thorsett, S. E., Arzoumanian, Z., Camilo, F. & Lyne, A. G. The Triple Pulsar System PSR B1620-26 in M4. *ApJ* **523**, 763–770 (1999). [arXiv:astro-ph/9903227](https://arxiv.org/abs/astro-ph/9903227).
8. Sigurdsson, S., Richer, H. B., Hansen, B. M., Stairs, I. H. & Thorsett, S. E. A Young White Dwarf Companion to Pulsar B1620-26: Evidence for Early Planet Formation. *Science* **301**, 193–196 (2003). [arXiv:astro-ph/0307339](https://arxiv.org/abs/astro-ph/0307339).
9. Bhattacharya, D. & van den Heuvel, E. P. J. Formation and evolution of binary and millisecond radio pulsars. *Phys. Rep.* **203**, 1–124 (1991).
10. Boyles, J. *et al.* The Green Bank Telescope 350 MHz Drift-scan survey. I. Survey Observations and the Discovery of 13 Pulsars. *ApJ* **763**, 80 (2013). [1209.4293](https://arxiv.org/abs/1209.4293).
11. Lynch, R. S. *et al.* The Green Bank Telescope 350 MHz Drift-scan Survey II: Data Analysis and the Timing of 10 New Pulsars, Including a Relativistic Binary. *ApJ* **763**, 81 (2013). [1209.4296](https://arxiv.org/abs/1209.4296).
12. Wolszczan, A. & Frail, D. A. A planetary system around the millisecond pulsar PSR1257+12. *Nature* **355**, 145–147 (1992).

13. Wolszczan, A. Confirmation of Earth-Mass Planets Orbiting the Millisecond Pulsar PSR B1257+12. *Science* **264**, 538–542 (1994).
14. Backer, D. C. & Hellings, R. W. Pulsar timing and general relativity. *ARA&A* **24**, 537–575 (1986).
15. Peale, S. J. On the verification of the planetary system around PSR 1257+12. *AJ* **105**, 1562–1570 (1993).
16. Abazajian, K. N. *et al.* The Seventh Data Release of the Sloan Digital Sky Survey. *ApJS* **182**, 543–558 (2009). 0812.0649.
17. Portegies Zwart, S., van den Heuvel, E. P. J., van Leeuwen, J. & Nelemans, G. The Formation of the Eccentric-orbit Millisecond Pulsar J1903+0327 and the Origin of Single Millisecond Pulsars. *ApJ* **734**, 55 (2011). 1103.2375.
18. Champion, D. J. *et al.* An Eccentric Binary Millisecond Pulsar in the Galactic Plane. *Science* **320**, 1309–1312 (2008). 0805.2396.
19. Freire, P. C. C. *et al.* On the nature and evolution of the unique binary pulsar J1903+0327. *MNRAS* **412**, 2763–2780 (2011). 1011.5809.
20. Mardling, R. A. New developments for modern celestial mechanics - I. General coplanar three-body systems. Application to exoplanets. *MNRAS* **435**, 2187–2226 (2013). 1308.0607.
21. Ford, E. B., Kozinsky, B. & Rasio, F. A. Secular Evolution of Hierarchical Triple Star Systems. *ApJ* **535**, 385–401 (2000).
22. Larwood, J. D. & Papaloizou, J. C. B. The hydrodynamical response of a tilted circumbinary disc: linear theory and non-linear numerical simulations. *MNRAS* **285**, 288–302 (1997). arXiv:astro-ph/9609145.
23. Tauris, T. M. & Savonije, G. J. Formation of millisecond pulsars. I. Evolution of low-mass X-ray binaries with  $P_{\text{orb}} > 2$  days. *A&A* **350**, 928–944 (1999). arXiv:astro-ph/9909147.
24. Özel, F., Psaltis, D., Narayan, R. & Santos Villarreal, A. On the Mass Distribution and Birth Masses of Neutron Stars. *ApJ* **757**, 55 (2012). 1201.1006.
25. Lattimer, J. M. The Nuclear Equation of State and Neutron Star Masses. *Annual Review of Nuclear and Particle Science* **62**, 485–515 (2012). 1305.3510.
26. Will, C. M. The Confrontation between General Relativity and Experiment. *Living Reviews in Relativity* **9**, 3 (2006). arXiv:gr-qc/0510072.
27. Freire, P. C. C., Kramer, M. & Wex, N. Tests of the universality of free fall for strongly self-gravitating bodies with radio pulsars. *Classical and Quantum Gravity* **29**, 184007 (2012). 1205.3751.

28. Stairs, I. H. *et al.* Discovery of Three Wide-Orbit Binary Pulsars: Implications for Binary Evolution and Equivalence Principles. *ApJ* **632**, 1060–1068 (2005). [astro-ph/0506188](#).
29. Gonzalez, M. E. *et al.* High-precision Timing of Five Millisecond Pulsars: Space Velocities, Binary Evolution, and Equivalence Principles. *ApJ* **743**, 102 (2011). [1109.5638](#).
30. Kurucz, R. ATLAS9 Stellar Atmosphere Programs and 2 km/s grid. *ATLAS9 Stellar Atmosphere Programs and 2 km/s grid. Kurucz CD-ROM No. 13. Cambridge, Mass.: Smithsonian Astrophysical Observatory, 1993.* **13** (1993).

**Acknowledgements** We thank D. Levitan and R. Simcoe for providing optical and infrared observations, J. Deneva for early Arecibo observations, P. Bergeron for use of his white dwarf photometry models; K. O’Neil and F. Camilo for approving discretionary time observations on the GBT and Arecibo, respectively, J. Heyl, E. Algol, and P. Freire for discussions, and G. Kuper, J. Sluman, Y. Tang, G. Jozsa, and R. Smits for their help supporting the WSRT observations. The GBT and VLBA are operated by the National Radio Astronomy Observatory, a facility of the National Science Foundation operated under cooperative agreement by Associated Universities, Inc. The Arecibo Observatory is operated by SRI International in alliance with Ana G. Méndez-Universidad Metropolitana and the Universities Space Research Association, under a cooperative agreement with the National Science Foundation. The WSRT is operated by the Netherlands Institute for Radio Astronomy (ASTRON). This paper made use of data from the WIYN Observatory at Kitt Peak National Observatory, National Optical Astronomy Observatory, which is operated by the Association of Universities for Research in Astronomy (AURA) under cooperative agreement with the National Science Foundation. This work is also based in part on observations made with the Spitzer Space Telescope, which is operated by the Jet Propulsion Laboratory, California Institute of Technology under a contract with NASA. I.H.S., V.M.K., M.H.v.K., and A.B. acknowledge support from NSERC. A.M.A. and J.W.T.H. acknowledge support from a Vrije Competitie grant from NWO. J.B., D.R.L., V.I.K., & M.A.M. were supported by a WV EPSCoR Research Challenge Grant. V.M.K. acknowledges support from CRAQ/FQRNT, CIFAR, Canada Research Chairs Program, and the Lorne Trottier Chair.

**Contributions** S.M.R., M.A.M., and D.R.L. were co-PIs of the GBT survey which found the pulsar, and all other other authors except D.L.K., M.H.v.K., A.T.D., S.C., and A.S.-R. were members of the survey team who observed and processed data. J.B. found the pulsar in the search candidates. S.M.R. identified the source as a triple, wrote follow-up proposals, observed with the GBT, phase-connected the timing solution, and wrote the manuscript. I.H.S. and J.W.T.H. performed timing observations, wrote follow-up proposals, and substantially contributed to the initial timing solution. A.M.A. developed the successful timing model and performed the numerical integrations and MCMC analyses. D.L.K. identified the optical counterpart and then with M.H.v.K. and A.S.-R. performed optical/IR observations and the multi-wavelength analysis. M.H.v.K. and D.L.K. both helped develop parts of the timing model. A.T.D. and S.C. performed the VLBA analysis. All authors contributed to interpretation of the data and the results and the final version of the manuscript.

**Competing Interests** The authors declare that they have no competing financial interests.

**Correspondence** Correspondence and requests for materials should be addressed to S.M.R. (email: [sransom@nrao.edu](mailto:sransom@nrao.edu)).

Parameter	Symbol	Value
Fixed values		
Right ascension	RA	$03^h 37^m 43^s .82589(13)$
Declination	Dec	$17^\circ 15' 14'' .828(2)$
Dispersion measure	DM	$21.3162(3) \text{ pc cm}^{-3}$
Solar system ephemeris		DE405
Reference epoch		MJD 55920.0
Observation span		MJD 55930.9 – 56436.5
Number of TOAs		26280
Weighted root-mean-squared residual		$1.34 \mu\text{s}$
Fitted parameters		
Spin-down parameters		
Pulsar spin frequency	$f$	$365.953363096(11) \text{ Hz}$
Spin frequency derivative	$\dot{f}$	$-2.3658(12) \times 10^{-15} \text{ Hz s}^{-1}$
Inner Keplerian parameters for pulsar orbit		
Semimajor axis projected along line of sight	$(a \sin i)_I$	$1.21752844(4) \text{ lt-s}$
Orbital period	$P_{b,I}$	$1.629401788(5) \text{ d}$
Eccentricity parameter ( $e \sin \omega$ ) <sub>I</sub>	$\epsilon_{1,I}$	$6.8567(2) \times 10^{-4}$
Eccentricity parameter ( $e \cos \omega$ ) <sub>I</sub>	$\epsilon_{2,I}$	$-9.171(2) \times 10^{-5}$
Time of ascending node	$t_{\text{asc},I}$	MJD 55920.407717436(17)
Outer Keplerian parameters for centre of mass of inner binary		
Semimajor axis projected along line of sight	$(a \sin i)_O$	$74.6727101(8) \text{ lt-s}$
Orbital period	$P_{b,O}$	$327.257541(7) \text{ d}$
Eccentricity parameter ( $e \sin \omega$ ) <sub>O</sub>	$\epsilon_{1,O}$	$3.5186279(3) \times 10^{-2}$
Eccentricity parameter ( $e \cos \omega$ ) <sub>O</sub>	$\epsilon_{2,O}$	$-3.462131(11) \times 10^{-3}$
Time of ascending node	$t_{\text{asc},O}$	MJD 56233.935815(7)
Interaction parameters		
Semimajor axis projected in plane of sky	$(a \cos i)_I$	$1.4900(5) \text{ lt-s}$
Semimajor axis projected in plane of sky	$(a \cos i)_O$	$91.42(4) \text{ lt-s}$
Inner companion mass over pulsar mass	$q_I = m_{cI}/m_p$	$0.13737(4)$
Difference in longs. of asc. nodes	$\delta_\Omega$	$2.7(6) \times 10^{-3} \text{ }^\circ$
Inferred or derived values		
Pulsar properties		
Pulsar period	$P$	$2.73258863244(9) \text{ ms}$
Pulsar period derivative	$\dot{P}$	$1.7666(9) \times 10^{-20}$
Inferred surface dipole magnetic field	$B$	$2.2 \times 10^8 \text{ G}$
Spin-down power	$\dot{E}$	$3.4 \times 10^{34} \text{ erg s}^{-1}$
Characteristic age	$\tau$	$2.5 \times 10^9 \text{ y}$
Orbital geometry		
Pulsar semimajor axis (inner)	$a_I$	$1.9242(4) \text{ lt-s}$
Eccentricity (inner)	$e_I$	$6.9178(2) \times 10^{-4}$
Longitude of periastron (inner)	$\omega_I$	$97.6182(19) \text{ }^\circ$
Pulsar semimajor axis (outer)	$a_O$	$118.04(3) \text{ lt-s}$
Eccentricity (outer)	$e_O$	$3.53561955(17) \times 10^{-2}$
Longitude of periastron (outer)	$\omega_O$	$95.619493(19) \text{ }^\circ$
Inclination of invariant plane	$i$	$39.243(11) \text{ }^\circ$
Inclination of inner orbit	$i_I$	$39.254(10) \text{ }^\circ$
Angle between orbital planes	$\delta_i$	$1.20(17) \times 10^{-2} \text{ }^\circ$
Angle between eccentricity vectors	$\delta_\omega \sim \omega_O - \omega_I$	$-1.9987(19) \text{ }^\circ$
Masses		
Pulsar mass	$m_p$	$1.4378(13) M_\odot$
Inner companion mass	$m_{cI}$	$0.19751(15) M_\odot$
Outer companion mass	8 $m_{cO}$	$0.4101(3) M_\odot$

**Table 1:** System parameters for PSR J0337+1715. Values in parentheses represent  $1\text{-}\sigma$  errors in the last decimal place(s), as determined by MCMC fitting (see Methods). The top section contains parameters supplied as input to our timing fit; the position was obtained from an observation with the VLBA, and the DM was measured from high-signal-to-noise Arecibo observations. The middle section contains the parameters used to describe the state of the system at the reference epoch – the initial conditions for the differential equation integrator. Along with the pulsar spin-down parameters, these parameters include the conventional Keplerian elements measurable in binary pulsars for each of the orbits, plus four parameters measurable only due to three-body interactions. These fourteen parameters can completely describe any configuration of three masses, positions, and velocities for which the center of mass remains fixed at the origin, provided that the longitude of the inner ascending node is zero. Although some fitting parameters are highly covariant, we computed all parameters and their errors based on the posterior distributions, taking into account these covariances. We use the standard formulae for computing  $B$ ,  $\dot{E}$ , and  $\tau$ , which assume a pulsar mass of  $1.4 M_{\odot}$  and a moment of inertia of  $10^{45} \text{ g cm}^2$ . We have not corrected these values for proper motion or Galactic acceleration. The Laplace-Lagrange parameters  $\epsilon_1$  and  $\epsilon_2$  parameterize eccentric orbits in a way that avoids a coordinate singularity at zero eccentricity. The pair  $(\epsilon_2, \epsilon_1)$  forms a vector in the plane of the orbit called the eccentricity vector. For a single orbit, the ascending node is the place where the pulsar passes through the plane of the sky moving away from us; the longitude of the ascending node specifies the orientation of the orbit on the sky. This is not measurable with the data we have, but the difference between the longitudes of the ascending nodes of the two orbits is measurable through orbital interactions. The invariant plane is the plane perpendicular to the total (orbital) angular momentum of the triple system.

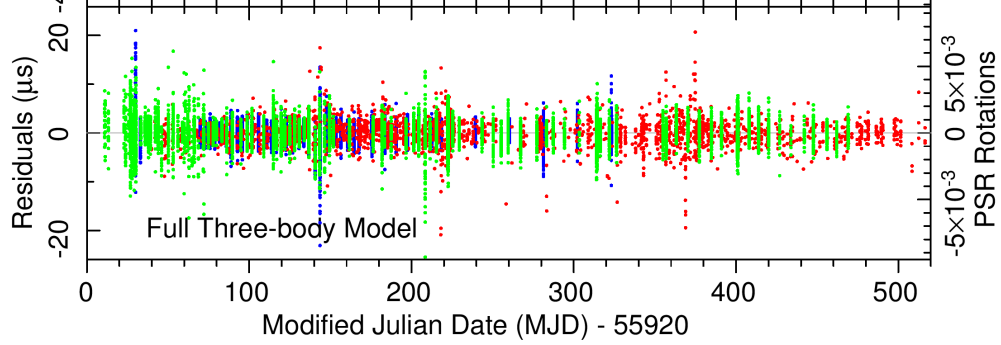
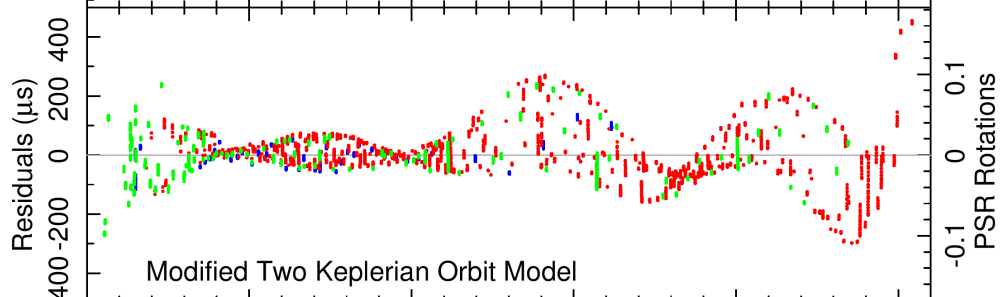
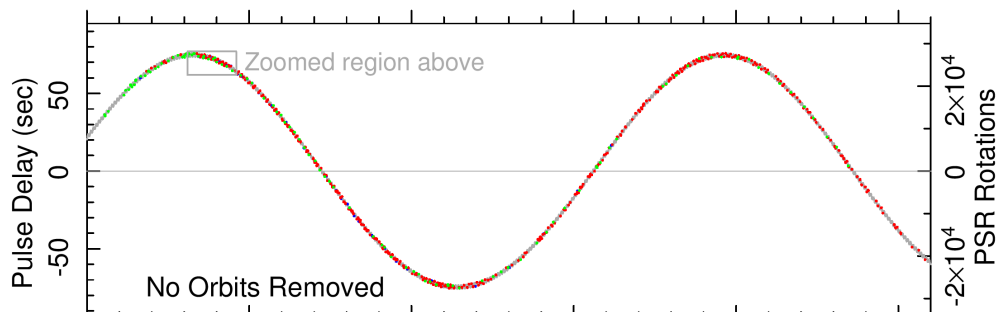
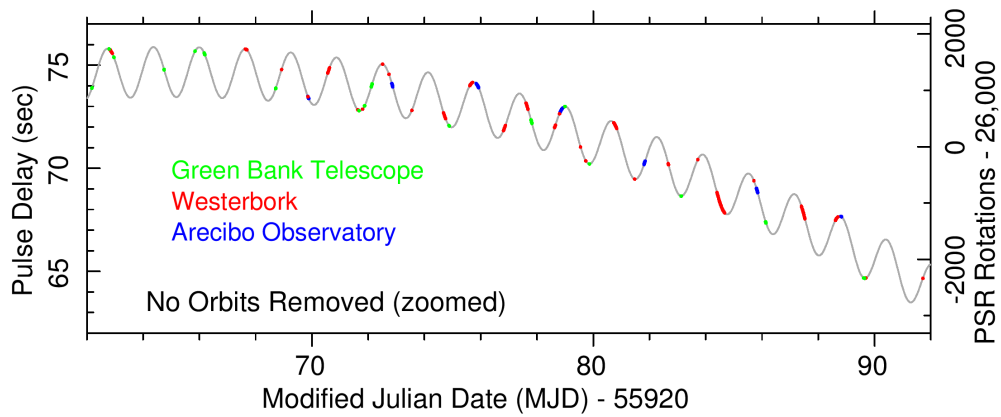


**Figure 1** Timing residuals and delays from the PSR J0337+1715 system. The top two panels show geometric light-travel time delays (that is, Rømer delays) in both time and pulse periods, across the inner (top panel) and outer (second panel down) orbits, and modified Julian dates (MJD) of radio timing observations from the GBT, WSRT, and the Arecibo telescope. Arrival time errors in these panels are approximately a million times too small to see. The third panel from the top shows the Newtonian three-body perturbations compared with the modified two-Keplerian-orbit model used for folding our data at the observed pulse period. The bottom panel shows the post-fit timing residuals from our full Markov chain Monte Carlo (MCMC)-derived three-body timing solution described in Table 1. The weighted root mean squared value of the 26,280 residuals is  $1.34 \mu\text{s}$ .

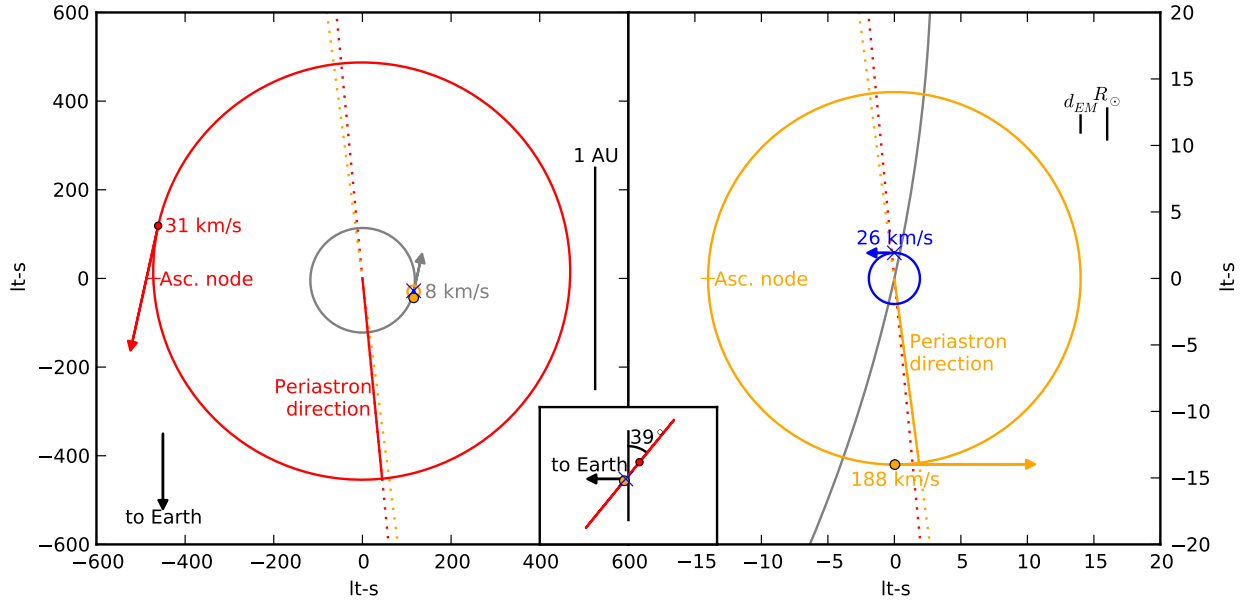


**Figure 2** Geometry of the PSR J0337+1715 system at the reference epoch. The left panel shows the orbital shape and velocity of the outer white dwarf (red) and the orbital shape and velocity of the centre of mass of the inner binary (grey). The right panel shows the orbital shapes and velocities of the inner white dwarf (orange) and pulsar (blue). Dotted red and orange lines indicate the directions of periastron for the inner and outer white dwarf orbits, respectively. The white dwarf positions when the pulsar or inner orbit center of mass crosses the ascending nodes are indicated. Vertical lines show length scales in the system in Astronomical Units (AU; left), or the Earth-Moon distance and the Solar radius ( $d_{EM}$  and  $R_{\odot}$ ; right). The inset plot at bottom centre shows the inclination of the basically coplanar orbits with respect to the Earth-pulsar direction.

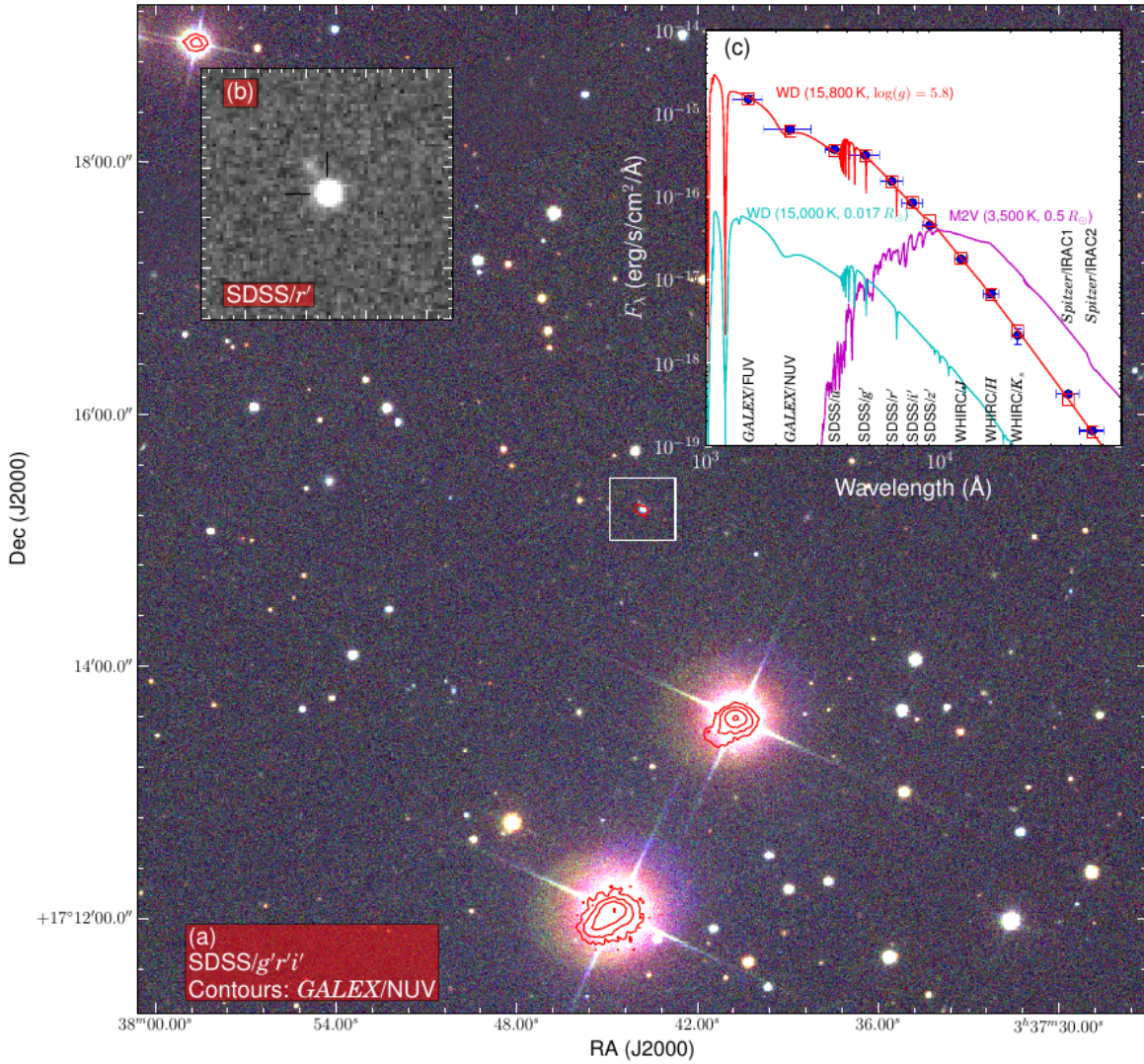


**Figure 3** Optical, infrared and ultraviolet data on PSR J0337+1715. The main panel (a) is a 3-colour optical image around J0337+1715, from the Sloan Digital Sky Survey (Methods). The contours are Galaxy Evolution Explorer (*GALEX*) near-ultraviolet (NUV) data. The box at the centre is the area of the inset in the upper-left (b), which shows a  $30'' \times 30''$  region of the SDSS  $r'$  filter (SDSS/ $r'$ ) image along with the VLBA position indicated by the tick marks. The inset in the upper-right (c) shows the spectral energy distribution. The data from *GALEX*, SDSS, the WIYN High Resolution Infrared Camera (WHIRC) and the Spitzer Infrared Array Camera (IRAC) are the blue circles, as labelled. The error bars represent  $1\sigma$  uncertainties in the  $y$  direction (flux density) and the widths of the photometric filters in the  $x$  direction (wavelength). The red curve is a model atmosphere consistent with our spectroscopic determination for the inner white dwarf (WD)

companion. The red boxes are the model atmosphere integrated through the appropriate filter passbands. For comparison, we also plot two possible models for the outer companion: a M2V star<sup>30</sup> (magenta) and a  $0.4 M_{\odot}$  white dwarf (cyan). All models have been reddened with an extinction of  $A_V = 0.44$  mag. The photometry is consistent with the light from the hot inner white dwarf (with a surface gravity  $\log(g)=5.8$ ) and a smaller and more massive outer white dwarf, but not a low-mass main-sequence star.

## Methods

**Radio timing observations.** Continuing timing observations over most of the past two years have been undertaken with Arecibo every few weeks, the GBT every week to 10 days, and the WSRT nearly daily, providing complementary timing precision and cadence. Without a complete timing solution, nor even a rough estimate of outer orbit parameters for most of the duration, the rapid cadence was essential to maintain unambiguous count of the pulsar’s rotations. Similar centre frequencies (1,440 MHz / 1,500 MHz), effective bandwidths ( $\sim 600$  MHz /  $\sim 700$  MHz) and observing systems (PUPPI / GUPPI)<sup>31</sup> are used at Arecibo and the GBT, respectively, while at the WSRT, the PUMAI instrument<sup>32</sup> is used with  $\sim 160$  MHz of bandwidth centred at 1,380 MHz. In all cases the data are coherently de-dispersed<sup>33</sup> at the pulsar’s dispersion measure ( $21.3162(3)$  pc cm<sup>-3</sup>) and folded modulo estimates of the predicted apparent pulsar spin period, initially determined from a polynomial expansion of inner orbital parameters re-fit on a weekly to monthly basis.

Pulse times of arrival (TOAs), determined by cross-correlating high signal-to-noise template profiles with folded pulse profiles using standard practices<sup>34</sup>, are measured every 10 seconds to 10 minutes depending on the telescope. We use the precise VLBA position (see below) and TEMPO2<sup>35</sup> to convert the arrival times at the observatory locations to the Solar System barycentre using the JPL DE405 planetary system ephemeris.

**Timing fitting procedures and the three-body model.** High-precision three-body integrations determine the stellar masses and a nearly complete orbital geometry using only well-tested Newtonian gravity and special relativity. For each set of trial parameters, we compute the pulsar and companion masses, positions, and velocities, and then use Newtonian gravity to compute their accelerations. We evolve the system forward using a Bulirsch-Stoer differential equation solver<sup>36</sup> (using 80-bit floating-point precision with ODEINT in the Boost library), obtaining position accuracy (limited by roundoff and truncation errors) on the order of a meter. We then compute the Rømer and Einstein delays and use a spin-down model of the pulsar to produce a set of predicted TOAs, which we compare to the observed TOAs using a weighted sum of squared residuals.

Fits to the measured TOAs without obvious systematic residuals are impossible without the inclusion of the three-body interactions as well as the special-relativistic transverse Doppler effect. General relativity is, in general, unimportant in the fitting of the system, but we calculate the full Einstein and Shapiro delays<sup>14</sup> based on the determined system masses and geometry and incorporate them into the resulting best-fit parameters. Ignoring these effects would lead to a distortion of orbital parameters, particularly the projected semimajor axes, as the delays would be absorbed into

the fit. The magnitude of the Shapiro delay is  $\sim 2.9 \mu\text{s}$  and  $\sim 5.8 \mu\text{s}$  peak-to-peak over the inner and outer orbits, respectively.

The parameter space is explored using Markov chain Monte Carlo techniques<sup>37</sup>, and the parameter values given in Table 1 are the Bayesian posterior expected values. We also use the posterior distribution to compute the standard deviations, quoted as 1-sigma uncertainties. This process marginalizes over covariances between parameters and derived values.

**Ultraviolet, optical, and infrared observations.** After we identified J0337+1715 in the SDSS Data Release 7<sup>16</sup>, we identified the same object as an ultraviolet source in the *GALEX* All-sky Imaging Survey<sup>38</sup>, confirming the blue colours (Figure 3). We obtained further near-infrared photometry with the WHIRC imager<sup>39</sup> on the Wisconsin Indiana Yale NOAO (WIYN) 3.5-m telescope and mid-infrared photometry with the post-cryogenic Infrared Array Camera (IRAC) onboard the *Spitzer Space Telescope*<sup>40</sup>.

We fit the data using synthetic WD photometry<sup>41</sup> (extended to *GALEX* bands by P. Bergeron, personal communication), finding extinction  $A_V = 0.34 \pm 0.04$  mag and effective temperature  $T_{\text{eff}}=14,600\pm 400$  K, with  $\chi^2 = 7.7$  for 9 degrees of freedom (Figure 3 inset (c)). This is close to the effective temperature we determined via optical spectroscopy (D.L.K. *et al.*, manuscript in preparation),  $T_{\text{eff,spec}}=15,800\pm 100$  K. Radial velocity measurements from those spectroscopic observations confirm that the optical star is the inner WD in the system. Given the spectroscopy-determined temperature and surface gravity of  $\log g=5.82\pm 0.05$ , and a radius of  $0.091\pm 0.005 R_{\odot}$  based on the WD mass from pulsar timing ( $0.197 M_{\odot}$ ), the synthetic photometry provides a photometric distance to the system of  $1,300\pm 80$  pc. That distance is somewhat larger than the  $\sim 750$  pc implied by the measured DM toward the pulsar and the NE2001 Galactic free electron density model<sup>42</sup>, although the latter likely has a large error range.

The photometry we measure is fully consistent with expectations for the inner companion only, as seen in Figure 3. No additional emission is needed over the 1,000–50,000 Å range, although only where we actually have spectra can we be certain that no other emission is present. Given its known mass of  $0.4 M_{\odot}$ , if the outer companion were a main-sequence star we would expect a spectral type of roughly M2V<sup>43</sup>, implying an effective temperature near 3,500 K and a radius of  $0.5 R_{\odot}$ . Figure 3 shows such a stellar model<sup>30</sup>, which exceeds the near-IR and mid-IR data-points by a factor of  $>5$ , ruling out a main-sequence star as the outer companion. Two main-sequence  $0.2 M_{\odot}$  stars would also cause an excess in the near- and mid-IR by a factor of  $\sim 2$ . Instead we find that a  $0.4 M_{\odot}$  WD with effective temperature  $< 20,000$  K (using synthetic photometry<sup>41</sup> again) is almost certainly the outer companion: such an object with  $\log(g)=7.5$  and radius  $0.018 R_{\odot}$  leads to a change in the  $\chi^2$  of 1 compared to the fit for only a single photosphere. An example of such an outer companion is also shown in Figure 3.

**Very Long Baseline Array Observations.** The position of J0337+1715 used in the timing analysis was determined from a single 3-hour observation with the Very Long Baseline Array (VLBA) on 13 February 2013, the first in a series of astrometric observations which will ultimately pro-

vide a  $\sim 1\text{--}2\%$  parallax distance and transverse velocity for the system. Eight dual-polarization, 32 MHz wide subbands were sampled from within the range 1392–1712 MHz, avoiding strong sources of radio frequency interference (RFI). The bright source J0344+1559 was used as a primary phase reference source, and a phase referencing cycle time of 4.5 minutes (total cycle) was employed.

The multi-field correlation capability of the DiFX software correlator used at the VLBA<sup>44</sup> made it possible to inspect all catalogued sources from the NRAO VLA Sky Survey (NVSS)<sup>45</sup> which fell within the VLBA field of view; of the 44 such sources, 4 were detected by the VLBA and J033630.1+172316 was found to be a suitable secondary calibrator, with a peak flux density of 4 mJy/beam. The use of an “in-beam” secondary calibrator reduces the spatial and temporal interpolation of the calibration solutions and improves the (relative) astrometric precision substantially<sup>46</sup>. J0337+1715 was detected with a signal-to-noise ratio of 30, providing a formal astrometric precision of around 0.1 milli-arcsec.

The absolute positional accuracy of J0337+1715 in the International Celestial Reference Frame is currently limited by the registration of the position of J033630.1+172316 relative to J0344+1559; given the angular separation of  $2.3^\circ$  and the single observation, this is estimated at 1–2 milli-arcsec. This uncertainty in the absolute position will be reduced by additional VLBA observations. In addition to improving the absolute position and solving for parallax and proper motion, a full VLBA astrometric model will incorporate the  $237/D_{\text{kpc}}$   $\mu$ -arcsec reflex motion on the sky caused by the outer orbit, where  $D_{\text{kpc}}$  is the distance to the system in kpc.

31. DuPlain, R. *et al.* Launching GUPPI: the Green Bank Ultimate Pulsar Processing Instrument. In *Advanced Software and Control for Astronomy II*, vol. 7019 of *SPIE Conf. Series* (2008).
32. Karuppusamy, R., Stappers, B. & van Straten, W. PuMa-II: A Wide Band Pulsar Machine for the Westerbork Synthesis Radio Telescope. *PASP* **120**, 191–202 (2008).
33. Hankins, T. H. & Rickett, B. J. Pulsar signal processing. In Alder, B., Fernbach, S. & Rotenberg, M. (eds.) *Methods in Computational Physics. Volume 14 - Radio astronomy*, vol. 14, 55–129 (1975).
34. Taylor, J. H. Pulsar Timing and Relativistic Gravity. *Royal Society of London Philosophical Transactions Series A* **341**, 117–134 (1992).
35. Hobbs, G. B., Edwards, R. T. & Manchester, R. N. TEMPO2, a new pulsar-timing package - I. An overview. *MNRAS* **369**, 655–672 (2006). [astro-ph/0603381](https://arxiv.org/abs/astro-ph/0603381).
36. Bulirsch, R. & Stoer, J. Asymptotic upper and lower bounds for results of extrapolation methods. *Numerische Mathematik* **8**, 93–104 (1966).
37. Foreman-Mackey, D., Hogg, D. W., Lang, D. & Goodman, J. emcee: The MCMC Hammer. *PASP* **125**, 306–312 (2013). [1202.3665](https://arxiv.org/abs/1202.3665).

38. Morrissey, P. *et al.* The Calibration and Data Products of GALEX. *ApJS* **173**, 682–697 (2007).
39. Meixner, M. *et al.* Design Overview and Performance of the WIYN High Resolution Infrared Camera (WHIRC). *PASP* **122**, 451–469 (2010).
40. Fazio, G. G. *et al.* The Infrared Array Camera (IRAC) for the Spitzer Space Telescope. *ApJS* **154**, 10–17 (2004).
41. Tremblay, P.-E., Bergeron, P. & Gianninas, A. An Improved Spectroscopic Analysis of DA White Dwarfs from the Sloan Digital Sky Survey Data Release 4. *ApJ* **730**, 128 (2011). 1102.0056.
42. Cordes, J. M. & Lazio, T. J. W. NE2001. I. A New Model for the Galactic Distribution of Free Electrons and its Fluctuations (2002). astro-ph/0207156.
43. Cox, A. N. *Allen's Astrophysical Quantities* (AIP Press/Springer, New York, 2000), 4 edn.
44. Deller, A. T. *et al.* DiFX-2: A More Flexible, Efficient, Robust, and Powerful Software Correlator. *PASP* **123**, 275–287 (2011).
45. Condon, J. J. *et al.* The NRAO VLA Sky Survey. *AJ* **115**, 1693–1716 (1998).
46. Chatterjee, S. *et al.* Precision Astrometry with the Very Long Baseline Array: Parallaxes and Proper Motions for 14 Pulsars. *ApJ* **698**, 250–265 (2009).